Effects of Cane Density on Floricane Raspberry Assessed Using UAV-Based Multispectral Imaging

Kamil Buczyński * and Magdalena Kapłan

Posted Date: 16 April 2026

doi: 10.20944/preprints202604.1152.v1

Keywords: *Rubus*; berry; drone; unmanned aerial vehicle; remote sensing

 doi:10.20944/preprints202604.1152.v1

Article

Effects of Cane Density on Floricane Raspberry Assessed Using UAV-Based Multispectral Imaging

Kamil Buczyński * and Magdalena Kapłan

Institute of Horticulture Production, University of Life Science in Lublin, 28 Głęboka, 20-612 Lublin, Poland

* Correspondence: kamil.buczynski@up.edu.pl

Abstract

This study addresses the role of cane density as a key agronomic factor in floricane raspberry production and explores its relationship with canopy structure assessed using UAV-based multispectral imaging. Although cane density is widely recognized as critical for yield formation, its interaction with remotely sensed vegetation indices remains insufficiently understood. The experiment was conducted in an open-field plantation in eastern Poland using four floricane raspberry cultivars and four cane-density treatments (two to five canes per plant). Yield components were measured throughout the harvest period, and multispectral data were acquired using an unmanned aerial vehicle to derive vegetation indices and assess spatial and temporal canopy variability. Yield per plant and fruit number increased consistently with cane density, while yield per cane decreased, indicating a trade-off between individual cane productivity and total yield. Fruit size remained relatively stable and was primarily influenced by harvest timing. Vegetation indices followed a common seasonal pattern, with moderate and variable responses to cane density. The integration of yield measurements with multispectral data revealed that cane density influences not only productivity but also canopy structure and its spatial uniformity. These findings highlight the potential of combining agronomic practices with remote sensing approaches to support data-driven optimization of raspberry production systems.

Keywords: *Rubus*; berry; drone; unmanned aerial vehicle; remote sensing

1. Introduction

Berries are increasingly recognized as functional foods with high nutritional value and associated health benefits, which has contributed to growing consumer demand and expansion of their production [1]. The *Rubus L.* genus including raspberries and blackberries constitutes an important resource with potential benefits for human health, and its broader cultivation and utilization may contribute significantly to improving global nutrition and public health outcomes [2]. Raspberry is one of the most widely cultivated berry crops globally, with production levels showing a continuous upward trend [3]. In *Rubus* species, the perennial plant structures include the root collar and the root system. In floricane cultivars, the cane life cycle extends over two growing seasons. During the first season, canes undergo elongation while remaining vegetative, whereas in the second season, lateral buds differentiate into short fruiting laterals that produce inflorescences. After fruiting, the canes senesce and die [4]. The architectural structure, growth vigor, cane diameter, and internode length of raspberry shrubs are characteristic traits specific to each cultivar. In addition, cultivars vary in the number of canes arising from the root collar and in their capacity to produce root suckers [5]. Shrubs of *Rubus idaeus* L. are characterized by the production of numerous root suckers [4], which necessitates the regulation of cane density to maintain optimal conditions for plant development. Pruning represents a critical cultivation practice in raspberry production, playing an important role in regulating fruit load, limiting disease incidence, and improving fruit quality [6]. The raspberry production industry is progressively extending into a wide range of climatic conditions and cultivation systems to ensure a year-round supply of high-quality fruit. Achieving

 doi:10.20944/preprints202604.1152.v1

this objective while maintaining high productivity requires the implementation of agronomic practices that regulate plant growth and development from the nursery stage [7]. Moreover, the continuous introduction of new raspberry cultivars necessitates the optimization of cane density for each genotype, thereby driving the implementation of new technologies to support this process.

Modern precision agriculture approaches are based on the systematic collection of high-quality data, which can be efficiently acquired using unmanned aerial systems (UAS) [8]. The monitoring of crop conditions constitutes a fundamental component of sustainable agricultural systems and food security, especially in the context of escalating challenges related to climate change and environmental degradation [9]. Improving the efficiency of agricultural production is widely recognized as a fundamental approach to securing global food supplies in the 21st century. The advancement toward Agriculture 5.0 necessitates the adoption of innovative technologies that support higher productivity, mitigate environmental impacts, and contribute to resolving critical social and political issues associated with modern food systems [10]. Digitalization in agriculture presents significant potential for both economic optimization and the advancement of sustainable practices. Within this framework, Agriculture 5.0 emphasizes the transition from data collection to the development of actionable knowledge supporting real-world decision-making [11].

Remote sensing methods are applied in a broad range of disciplines, enabling the acquisition of diverse and accessible datasets using different types of technologies such as RGB and multispectral sensors [12]. Image analysis constitutes a fundamental approach for the detection, differentiation, and quantification of various types of imagery, including grayscale, color, and multispectral data composed of several discrete spectral bands, typically fewer than ten [13]. Unmanned Aerial Vehicle (UAV), commonly referred to as drones, have undergone rapid development in recent decades. In the agricultural sector, their adoption has transformed farming practices by enabling cost reduction, improving operational efficiency, and enhancing overall economic performance [14]. Multispectral sensors mounted on unmanned aerial vehicles are widely applied in crop health assessment. The use of the same imaging systems for close-range data acquisition can further enhance the accuracy of crop condition evaluation. In contrast to RGB cameras, which are limited to the visible spectrum, multispectral sensors capture additional spectral bands, enabling more detailed analysis of plant status [15]. The integration of UAV-based monitoring with advanced machine learning techniques and IoT sensors has emerged as a key approach for real-time surveillance in agricultural systems [16]. The Internet of Things (IoT), together with advanced data analytics, represents a leading component of the ongoing technological transformation, enabling substantial improvements in real-time monitoring and decision-making processes aimed at optimizing agricultural productivity. As agriculture increasingly adopts a data-driven and digital paradigm, a comprehensive understanding of IoT and analytical applications becomes essential [17].

The application of multispectral imaging and UAV-based technologies in raspberry production remains at an early stage of adoption. At the same time, the regulation of cane density continues to be a key agronomic practice in modern raspberry cultivation, requiring ongoing adjustment due to the continuous introduction of new cultivars. Accordingly, this study aimed to assess the impact of cane density on yield in floricane raspberry cultivars, integrating vegetation indices derived from UAV-acquired multispectral data.

2. Materials and Methods

2.1. Overview of the Research Area

The study was conducted in an open-field raspberry plantation established in May 2023 in eastern Poland within the Lublin Upland macroregion (51°11′ N, 21°49′ E). The plantation was established using plug plants on soil classified as class IIIa according to the Polish soil valuation system. The experiment included four floricane raspberry cultivars (Table 1.)

Table 1. Overview of the cultivars used in the experiment.

 doi:10.20944/preprints202604.1152.v1

Cultivar	Country of origin	Breeding program
Przehyba	Poland	Sadowniczy Zakład Doświadczalny Brzezna
Glen Ample	Scotland	James Hutton Institute
Glen Carron	Scotland	James Hutton Institute
Glen Mor	Scotland	James Hutton Institute

The experiment was arranged in rows oriented along the east–west direction, with a spacing of 3.0 m between rows (Figure 1). Within each cultivar, four cane density treatments were established, resulting in a total of eight experimental combinations. Depending on the treatment, two to five canes were retained per plant in order to evaluate the effect of cane number on yield and fruit quality.

Figure 1. Experimental plantation.

Each treatment combination included 18 plants organized into three replicates of six plants each. Plants were spaced at 0.40 m within the row, corresponding to a planting density of 8000 plants ha^{-1}. The replicate was considered the experimental unit, and all yield measurements were recorded at this level.

Under typical raspberry production conditions, plants are managed as continuous hedgerows, where canes from neighboring plants form a uniform canopy structure. This limits the possibility of assigning yield parameters to individual plants without disturbing the canopy. For this reason, measurements were performed on groups of adjacent plants, which allowed the evaluation of treatment effects under field conditions while preserving natural canopy architecture.

Cane number was adjusted in the second half of May, after the risk of spring frost had passed, allowing the selection of well-developed and undamaged shoots. No yield measurements were conducted in 2024, as plants were still in the establishment phase and produced a limited number of canes, which is typical for the first year after planting.

Crop management followed integrated pest management guidelines applicable in Poland. Fertilization was performed in accordance with current recommendations and adjusted to plant nutritional requirements, using a uniform scheme across all treatments. Irrigation was provided through a drip system consisting of two lines with emitters of 1 L h^{-1} discharge spaced at 20 cm intervals, which supported stable plant growth under variable moisture conditions.

Protection against sub-zero temperatures at the beginning of the growing season was achieved by covering entire rows with two layers of white non-woven fabric (23 g m^{-2}). As the season progressed, frost protection was provided using sprinklers, activated during frost events (Figure 2).

 doi:10.20944/preprints202604.1152.v1

Figure 2. Frost protection: (**a**) white non-woven fabric (**b**) water sprinkling.

Air temperature was monitored using a sensor (AGRONETPRO Sp. z o.o., Dęblin, Poland) installed at a height of 1 m within the experimental site. Figure 3 presents daily minimum, maximum, and mean air temperatures recorded during the 2025 growing season. Daily extremes are shown as shaded areas, while the mean temperature is indicated by a continuous line. Threshold values of 0 °C and 30 °C are marked with dashed lines, and monthly averages are provided for reference. In 2025, thermal conditions were characterized by considerable variability, particularly during the early stages of the growing season. The winter period showed alternating mild and cold intervals, with frequent occurrences of sub-zero temperatures, indicating potential exposure of plants to cold stress. As the season progressed, a gradual increase in temperature was observed, accompanied by moderate daily fluctuations. During the summer months, temperature conditions remained relatively stable, with only occasional exceedance of 30 °C. Overall, the 2025 growing season was defined by a variable early phase followed by a more stable thermal regime during the main period of plant development, which may have influenced growth dynamics and phenological responses.

 doi:10.20944/preprints202604.1152.v1

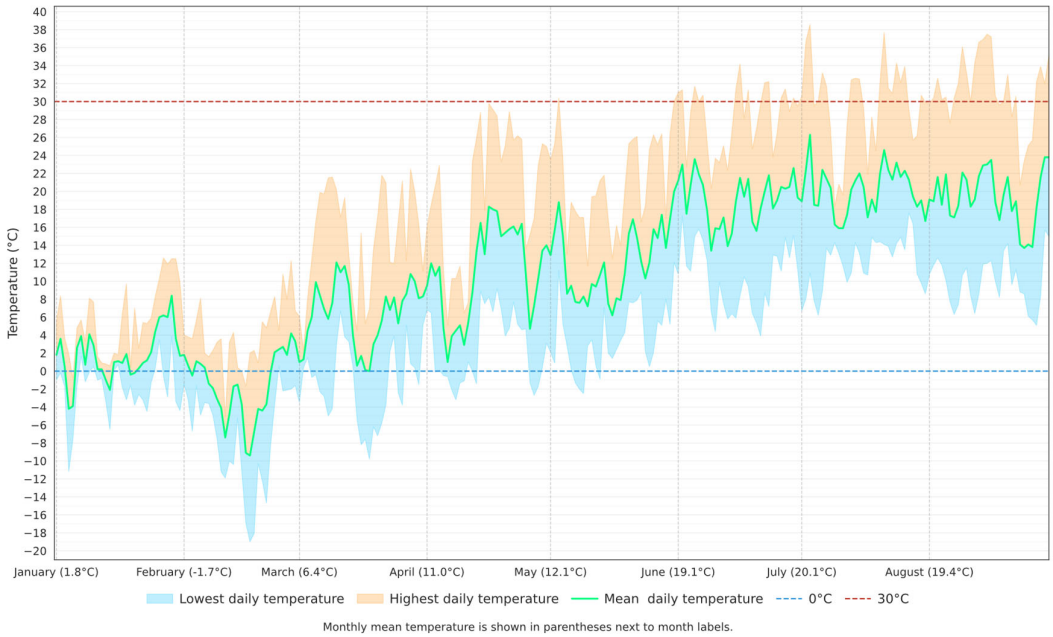

Figure 3. Temperature.

2.2. *Measurements*

2.2.1. Yield

Yield responses to cane density were assessed during the 2025 growing season. Fruits were harvested at intervals of one to three days, depending on ripening dynamics and weather conditions. All harvested fruits were weighed with an accuracy of 0.1 g using an electronic scale (Steinberg Systems SBS-LW-600, Expondo Polska sp. z o.o. sp.k, Zielona Góra, Poland). In addition, the number of fruits was recorded to enable the calculation of mean fruit weight.

2.2.2. Multispectral Imaging

Multispectral data were collected during the 2025 growing season using a DJI Mavic 3 Multispectral unmanned aerial vehicle (SZ DJI Technology Co., Ltd., Shenzhen, China) (Figure 4). The platform combines an RGB sensor (4/3-inch CMOS, 20 MP; 5280 × 3956 pixels) with a multispectral sensor (1/2.8-inch CMOS, 5 MP; 2592 × 1944 pixels). Reflectance was recorded in four spectral bands, including near-infrared (860 ± 26 nm), red edge (730 ± 16 nm), red (650 ± 16 nm), and green (560 ± 16 nm). The system is equipped with real-time kinematic positioning, enabling high-precision georeferencing of the acquired imagery [18]. In addition, an onboard light sensor measured incident solar radiation and stored this information in the image metadata. These data were used for radiometric correction during image processing, which improved the consistency of multispectral measurements over time.

 doi:10.20944/preprints202604.1152.v1

Figure 4. Drone DJI Mavic 3 Multispectral.

Multispectral data were acquired using two flight configurations differing in spatial resolution. The missions were performed at altitudes of approximately 30.4 m and 49.9 m above the take-off point, resulting in orthomosaic ground sampling distances of 1.40 cm and 2.30 cm per pixel, respectively. Both configurations were executed using consistent flight settings, including fixed image overlap, a constant flight direction, and speed adjusted to altitude. Real-time kinematic positioning was used to ensure accurate georeferencing of the imagery. Image acquisition was conducted with automatic white balance, while geometric correction was not applied in order to retain the original image geometry. Detailed flight parameters for each configuration are presented in Table 2.

Table 2. Drone imaging mission parameters.

Ortho GSD (cm/pixel)	1.40	2.30
Route altitude (m)	30.4	49.9
Speed (m/s)	1.3	2
Course angle (°)	111	111
Side overlap ratio (%)	70	70
Frontal overlap ratio (%)	90	90
Dewarping	Off	Off
White balance	Auto	Auto
RTK	On	On

Multispectral observations were carried out between 20 May and 12 July, covering the period from cane density adjustment to harvest. Data from the final harvest stage were excluded, as intensive vegetative growth of current-season canes dominated the row structure at that time. Measurements were collected for entire experimental plots without further subdivision. Plot boundaries were defined by concrete support posts, which were used to verify the spatial extent of each treatment during data processing. Image acquisition was performed at intervals of 6 to 10 days depending on weather conditions, resulting in a total of eleven measurement campaigns. Flights were conducted under conditions of high solar illumination with minimal cloud cover to ensure consistent data

 doi:10.20944/preprints202604.1152.v1

quality. The dataset included RGB and multispectral imagery (G, R, RE, and NIR) covering all treatment combinations. Examples of the acquired imagery are presented in Figure 5.

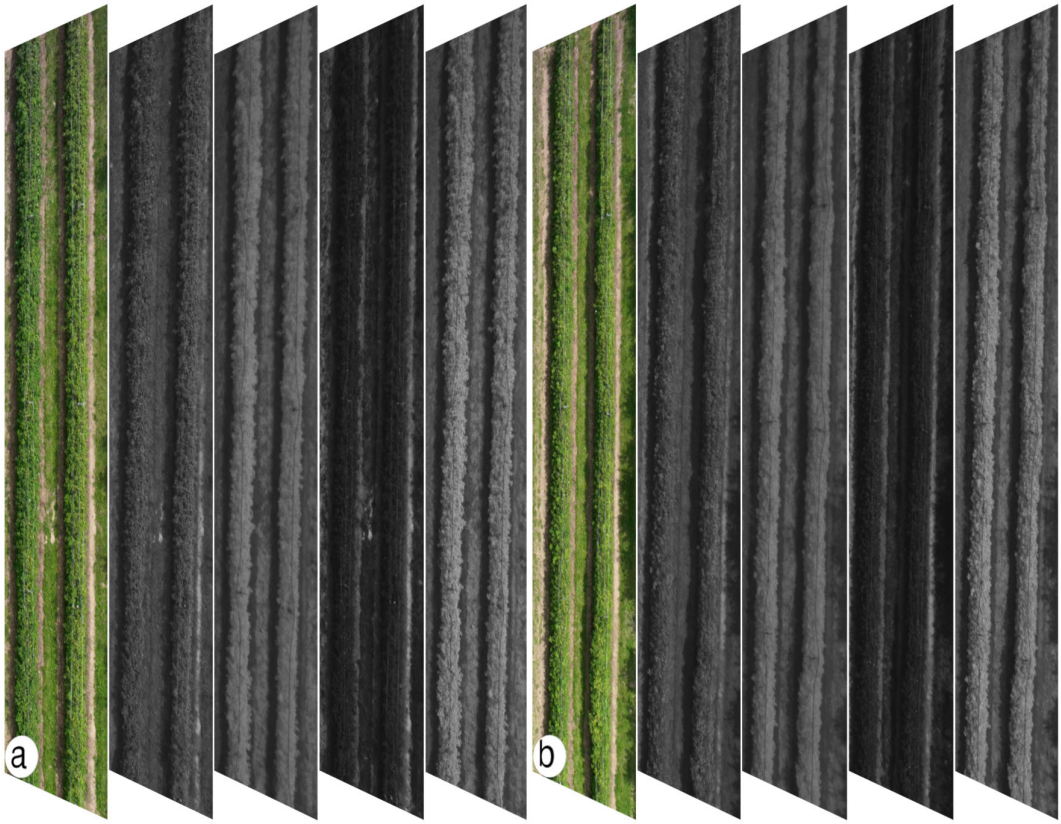

Figure 5. Remote sensing imagery of the experimental research area: (**a**) Glen Ample and Przehyba; (**b**) Glen Carron and Glen Mor.

UAV flights were performed between 11:00 and 13:00, when solar conditions ensured uniform illumination of the canopy and limited shading effects. Radiometric calibration was conducted before each flight using a calibrated reflectance panel (MicaSense, Inc., Seattle, USA). Image sequences were acquired with both RGB and multispectral sensors (G, R, RE, and NIR), with the panel positioned at heights of 0.6 m and 1.0 m above the take-off point. During calibration, both the reflectance panel and the onboard light sensor were exposed to direct illumination to ensure consistent radiometric correction.

2.3. *Analysis of Results*

2.3.1. Statistical Analysis

Statistical analysis was carried out in RStudio (Posit PBC, Boston, USA). The effects of experimental treatments on growth and yield variables were evaluated using one-way analysis of variance (ANOVA), with growing season included as a source of variation.

Model assumptions were checked prior to analysis. Residual normality was tested using the Shapiro–Wilk test, and homogeneity of variance was assessed with Levene's test. No significant deviations from these assumptions were observed.

Mean comparisons were performed using Tukey's honestly significant difference test. Results are presented as homogeneous groups indicated by letters, where identical letters denote no statistically significant differences. Lowercase letters refer to comparisons within columns, whereas

 doi:10.20944/preprints202604.1152.v1

uppercase letters indicate comparisons within rows. The *p*-values from the F-test are reported, and significance was set at $p \leq 0.05$.

Yield data were visualized using line and bar charts generated in PyCharm (JetBrains s.r.o., Amsterdam, Netherlands). A summary of the software environments, programming languages, and associated libraries used for data processing and visualization is provided in Table 3.

Table 3. Software.

Programming language R (4.4.0)	
Integrated development environment	Rstudio (2025.9.2.418)
Packages	readxl (1.4.5), dplyr (1.1.4), emmeans (2.0.1), multcomp (1.4.29), multcompView (0.1.10), circlize (0.4.17)
Programming language Python (3.12.0)	
Integrated development environment	PyCharm (2024.2.4, Community Edition)
Libraries	pandas (2.2.3), seaborn (0.13.2), matplotlib (3.9.2)

2.3.2. Multispectral Data Analysis

Multispectral data were processed using Pix4Dfields software (Pix4D S.A., Lausanne, Switzerland; version 2.12.0) with the Accurate processing workflow. This approach enabled the generation of high-resolution orthomosaics and elevation models, improving spatial accuracy and reducing geometric distortions, particularly in areas with variable terrain [19]. Radiometric correction was performed using a calibrated reflectance panel and incorporated information on sensor characteristics and illumination conditions, including incident solar radiation and sun position recorded by the onboard DLS sensor. GPU acceleration was applied to enhance processing efficiency. Orthomosaics were generated without pan-sharpening, and no limitations were imposed on ground sampling distance or output size, allowing processing at native resolution. Detailed processing parameters are provided in Table 4.

Table 4. Data processing settings.

Parameter	Setting
Processing pipeline	Accurate
reflectanceTargetUsed	True
enableRadiometry	True
enableGPU	True
orhtoMinGsd	0
orthoMaxSizeMPixels	0
enablePanSharpening	False
enableOrthoMinGsd	False
enableOrthoMaxSizeMPixels	False

Data processing parameters included adjustments for atmospheric conditions during each measurement, categorized as either clear or overcast. The specific settings applied for individual measurement campaigns are summarized in Table 5.

Table 5. Weather conditions during measurements.

Measurement №	Data	Processing settings
1	20.05	clear sky
2	26.05	clear sky

 doi:10.20944/preprints202604.1152.v1

3	04.06	over cast
4	10.06	overcast
5	18.06	clear sky
6	27.06	clear sky
7	02.07	clear sky
8	12.07	overcast

Pix4Dfields provides a range of annotation tools for image analysis. In this study, priority was given to methods that ensured efficient labeling while maintaining high data quality under hedgerow raspberry production conditions. Two annotation strategies were evaluated. The first, based on a bounded rectangular area, focused on the central portion of the hedgerow, which reduced the influence of soil background but resulted in partial exclusion of cane tips extending beyond the canopy. The second approach covered the full width of the hedgerow, ensuring inclusion of all plant material, although at the cost of increased background signal. Figure 6 presents the annotation methods used in this study.

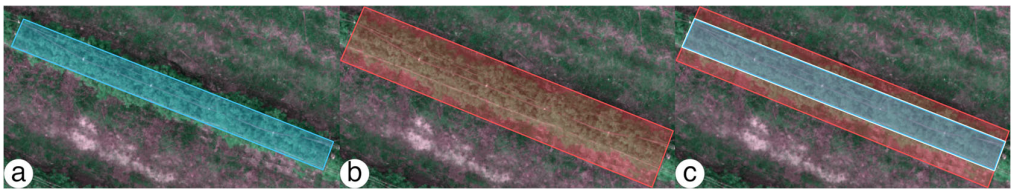

Figure 6. Annotation Methods: (**a**) Rectangle bounded; (**b**) Rectangle on the edges; (**c**) Comparison of Rectangle bounded and Rectangle on the edges.

Multispectral data analysis was based on the calculation of vegetation indices. The selected indices, commonly used in remote sensing, were derived according to their standard mathematical formulations. In these equations, NIR, R, G, and RE represent spectral reflectance in the near-infrared, red, green, and red-edge bands, respectively. The resulting layers generated during multispectral data processing are presented in Figure 7.

The Green Normalized Difference Vegetation Index (GNDVI) was used to characterize variability in vegetation condition. This index is based on the relationship between reflectance in the near-infrared and green spectral regions and is particularly sensitive to changes in chlorophyll content (Equation 1).

$$\mathrm{GNDVI} = \frac{\mathrm{NIR} - \mathrm{G}}{\mathrm{NIR} + \mathrm{G}} \quad (1)$$

The Normalized Difference Red Edge (NDRE) index was used to assess chlorophyll variability based on reflectance in the near-infrared and red-edge spectral regions. This index is particularly suitable for vegetation characterized by high canopy density (Equation 2).

$$\mathrm{NDRE} = \frac{\mathrm{NIR} - \mathrm{RE}}{\mathrm{NIR} + \mathrm{RE}} \quad (2)$$

Chlorophyll-related properties were further evaluated using the Modified Chlorophyll Absorption in Reflectance Index 2 (MCARI2), which enhances sensitivity to chlorophyll absorption while reducing the influence of canopy structure and soil background. This formulation includes a correction associated with leaf area index, representing the ratio of leaf area to ground surface (Equation 3).

$$\mathrm{MCARI2} = \frac{1.5[2.5(\mathrm{NIR} - \mathrm{R}) - 1.3(\mathrm{NIR} - \mathrm{G})]}{\sqrt{(2\mathrm{NIR} + 1)^2 - \left(6\mathrm{NIR} - 5\sqrt{\mathrm{R}}\right) - 0.5}} \quad (3)$$

 doi:10.20944/preprints202604.1152.v1

The Optimized Soil Adjusted Vegetation Index (OSAVI) was applied to account for soil background effects through the inclusion of a correction factor in the denominator. This index is particularly useful under conditions of sparse to moderate vegetation cover and partial canopy shading (Equation 4).

$$\mathrm{OSAVI} = \frac{\mathrm{NIR} - \mathrm{R}}{\mathrm{NIR} + \mathrm{R} + 0.16} \quad (4)$$

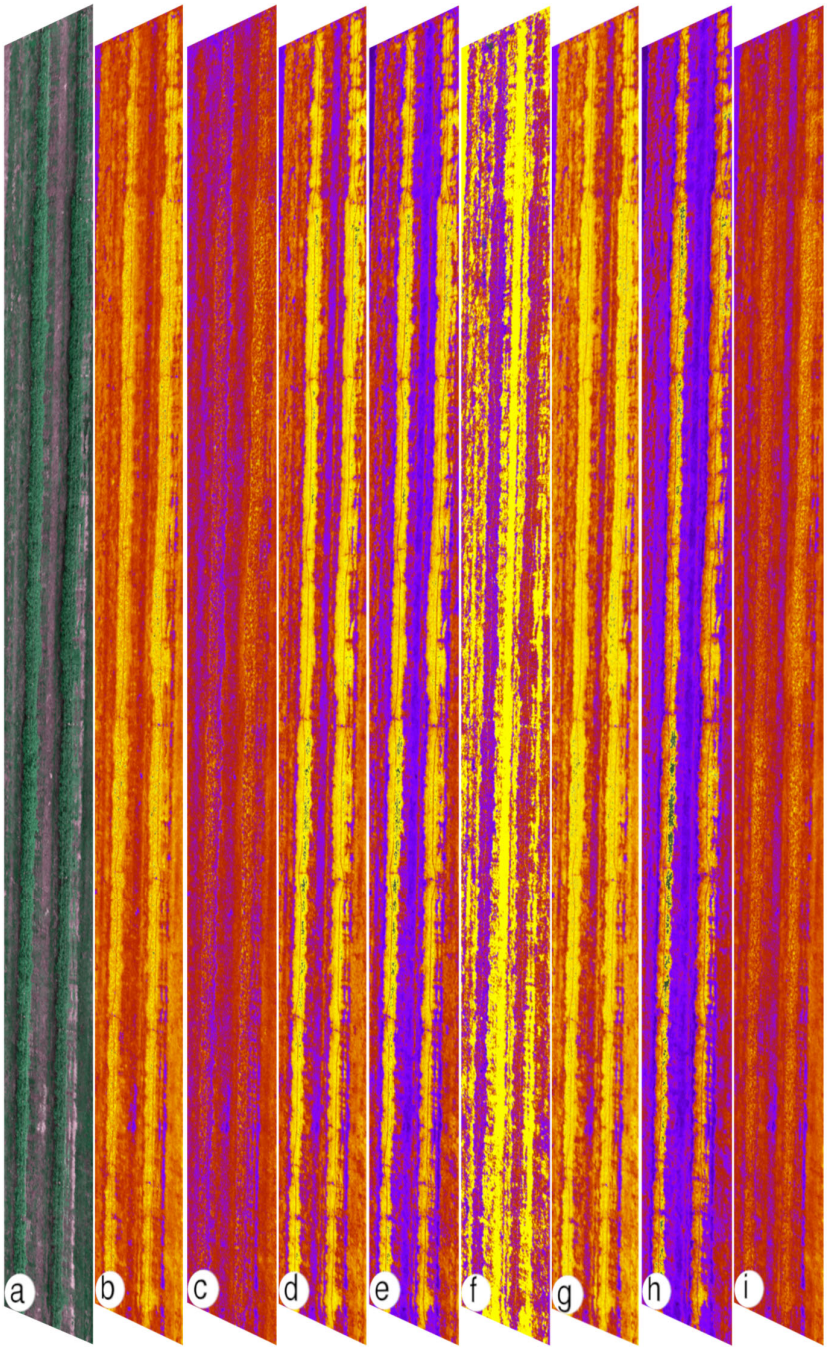

Figure 7. Layers: (**a**) Orthomosaic; (**b**) GNDVI; (**c**) NDRE; (**d**) OSAVI; (**e**) MCARI2; (**f**) SIPI2; (**g**) NDVI; (**h**) MCARI; (**i**) LCI.

 doi:10.20944/preprints202604.1152.v1

For each measurement date, datasets were organized according to cultivar, treatment combination, ground sampling distance, and annotation approach. Based on these data, the standard deviation (SD) and coefficient of variation (CV) of vegetation index values were calculated for all configurations, independently of measurement date. This analysis was used to evaluate the stability of different data processing configurations. As no single combination of ground sampling distance and annotation method consistently provided superior results across all indices and cultivars, a standardized approach was adopted. The bounded rectangle method was selected to limit the influence of background pixels, while a ground sampling distance of 1.40 cm per pixel was used due to its higher spatial resolution. Temporal dynamics of vegetation index values were analyzed using a Python-based script. To characterize these dynamics, a set of synthetic parameters was calculated and used for data presentation. These included the mean index value and the mean coefficient of variation, representing overall index level and data stability, respectively. Temporal patterns were further described by examining changes between consecutive measurement dates, including total amplitude, relative amplitude, and cumulative increases and decreases in index values. These metrics enabled assessment of the intensity and progression of vegetation index variation over time. Additionally, temporal patterns were characterized using the Roughness dynamics metric, which quantifies the irregularity of vegetation index trajectories over time. Lower values indicate more gradual and evenly distributed changes throughout the season, whereas higher values reflect concentration of variability within a limited number of measurement periods. The methodology applied for the analysis of results obtained in Pix4Dfields was based on an approach developed in a previous study [20,21].

Due to the large number of data combinations, defined as cultivar × treatment × vegetation index × ground sampling distance × annotation method, the complete dataset was not included in the main manuscript. This also applies to additional indices, including NDVI, MCARI, SIPI, and LCI, as well as the full set of derived metrics. Only representative and aggregated results are presented in this study, whereas the complete dataset, including raw outputs from Pix4Dfields, is available in a publicly accessible repository [22].

3. Results

3.1. Yield Parameters

Across all analysed cultivars, cane-number treatments exerted a strong and consistent effect on yield formation at the plant level.

Mean yield per plant increased progressively with increasing cane number for all cultivars. In each case, the lowest yields were observed in the two-cane treatments, while the highest yields were consistently associated with the five-cane combinations. Intermediate cane numbers formed clearly separated yield classes, resulting in a well-ordered response across the full range of treatments.

A similar pattern was observed for the mean number of fruits per plant. Fruit number increased monotonically with increasing cane number for all cultivars, closely mirroring the response of total yield. As with yield, two-cane treatments produced the fewest fruits per plant, whereas five-cane treatments consistently exhibited the highest fruit numbers, with intermediate treatments forming distinct and statistically separable groups.

In contrast, average fruit weight responded differently to cane-number treatments and showed cultivar-specific behaviour. For Glen Ample and Glen Carron, average fruit weight remained relatively stable across all cane-number combinations, with no clear differentiation among treatments. In Przehyba and Glen Mor, fruit weight exhibited a modest but significant reduction at higher cane numbers, with lower values observed in the four- and five-cane treatments compared with the lowest-density combinations.

Yield responses across cultivars were primarily driven by changes in fruit number rather than fruit size, while the effect of cane number on individual fruit weight was limited and cultivar-dependent.

 doi:10.20944/preprints202604.1152.v1

Table 6. Yield parameters.

Cultivar	Combination	Mean yield of 1 plant (g)	Mean number of fruits per plant (pcs.)	Average fruit weight (g)
Przehyba	Two canes	1,369.44 d	209.00 d	6.55 a
	Three canes	1,766.11 c	281.28 c	6.28 ab
	Four canes	2,061.10 b	334.00 b	6.17 b
	Five canes	2,275.58 a	369.61 a	6.16 b
	p-value	< 0.001	< 0.001	0.009
Glen Ample	Two canes	2,158.54 d	471.72 d	4.58 a
	Three canes	2,631.78 c	580.72 c	4.53 a
	Four canes	2,943.74 b	651.67 b	4.52 a
	Five canes	3,428.27 a	763.44 a	4.49 a
	p-value	< 0.001	< 0.001	0.914
Glen Carron	Two canes	1,704.64 c	453.29 d	3.76 a
	Three canes	2,089.89 b	559.38 c	3.74 a
	Four canes	2,278.01 b	618.62 b	3.68 a
	Five canes	2,528.13 a	689.14 a	3.67 a
	p-value	< 0.001	< 0.001	0.819
Glen Mor	Two canes	1,930.99 c	457.66 d	4.22 a
	Three canes	2,314.41 b	555.52 c	4.17 a
	Four canes	2,500.97 b	634.00 b	3.94 b
	Five canes	2,749.72 a	700.34 a	3.93 b
	p-value	< 0.001	< 0.001	0.004

The effect of cane number on yield per hectare and yield per cane is shown in Figure 8. Across all cultivars, yield per hectare increased consistently with increasing cane number. For each cultivar, the lowest hectare yields were associated with the two-cane treatments, while the highest yields were observed under the five-cane configuration. Intermediate cane numbers formed a clear progression between these extremes, resulting in a monotonic increase in yield per unit area across the full range of cane-number treatments.

In contrast, yield per cane exhibited an inverse response to cane number. For all cultivars, the highest yield per cane occurred in the two-cane treatments, followed by a systematic decline as cane number increased. The lowest per-cane yields were consistently observed in the five-cane combinations, indicating a clear trade-off between individual cane productivity and total yield per hectare. This opposing response of yield per hectare and yield per cane was consistent across all analysed cultivars, although the absolute magnitude of both metrics differed among cultivars.

 doi:10.20944/preprints202604.1152.v1

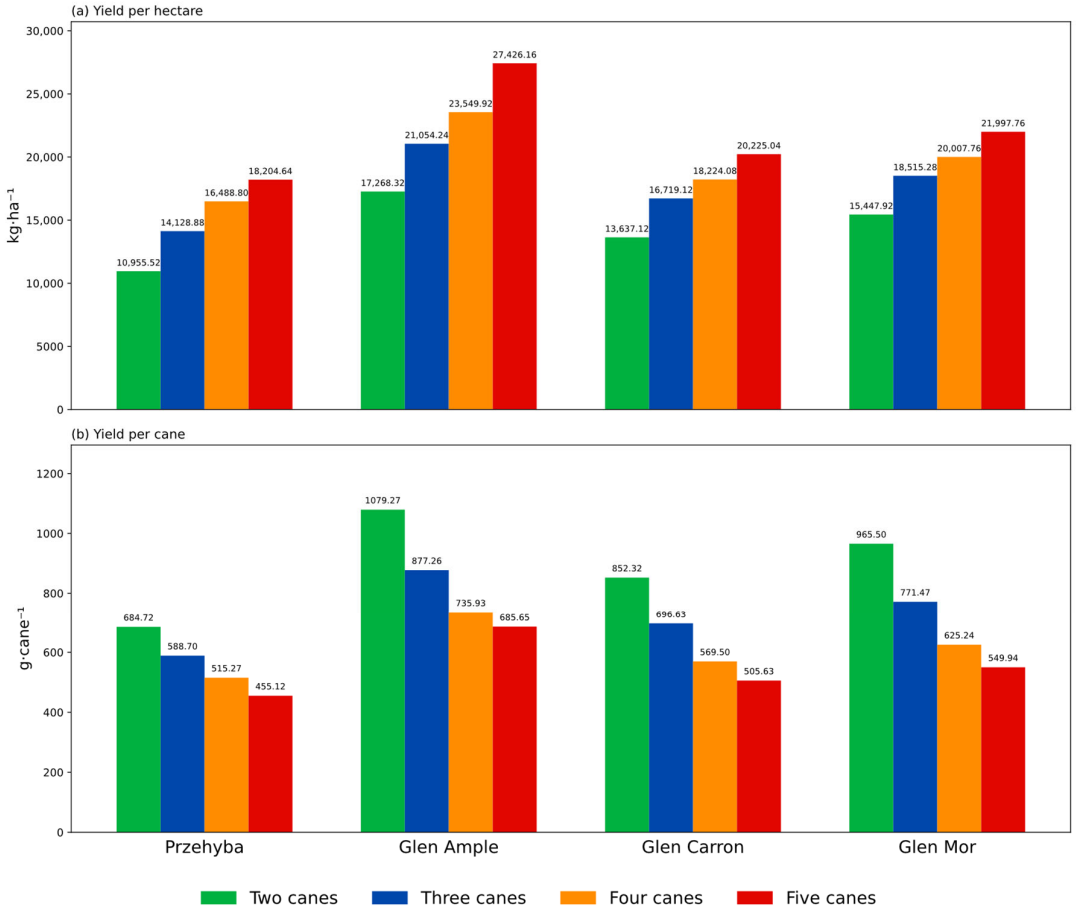

Figure 8. Yield: (a) per hectare; (b) per cane.

The distribution of yield across successive harvest dates, as influenced by cane number and cultivar, is shown in Figure 9. Across all cultivars, yield exhibited a strongly structured temporal pattern over successive harvests, characterised by a rapid increase during early harvests, followed by a pronounced mid-season maximum and a gradual decline towards the final harvests. This general temporal shape was consistent across cane-number treatments and cultivars, indicating a shared seasonal yield trajectory.

Cane-number treatments primarily affected the magnitude of yield rather than the timing of yield peaks. For all cultivars, higher cane-number combinations consistently produced higher yields across most harvests, with the five-cane treatment maintaining the highest yield levels throughout the season and the two-cane treatment remaining distinctly lower. Intermediate treatments (three and four canes) followed closely aligned trajectories between these extremes.

Despite differences in absolute yield levels, temporal fluctuations occurred synchronously across cane-number treatments within each cultivar. Peaks and declines in yield were aligned in time, suggesting that short-term yield variability was governed mainly by harvest timing rather than altering the relative separation among cane-number combinations.

Yield dynamics across harvests revealed a stable and repeatable hierarchy of cane-number treatments within each cultivar, superimposed on a common seasonal yield pattern.

 doi:10.20944/preprints202604.1152.v1

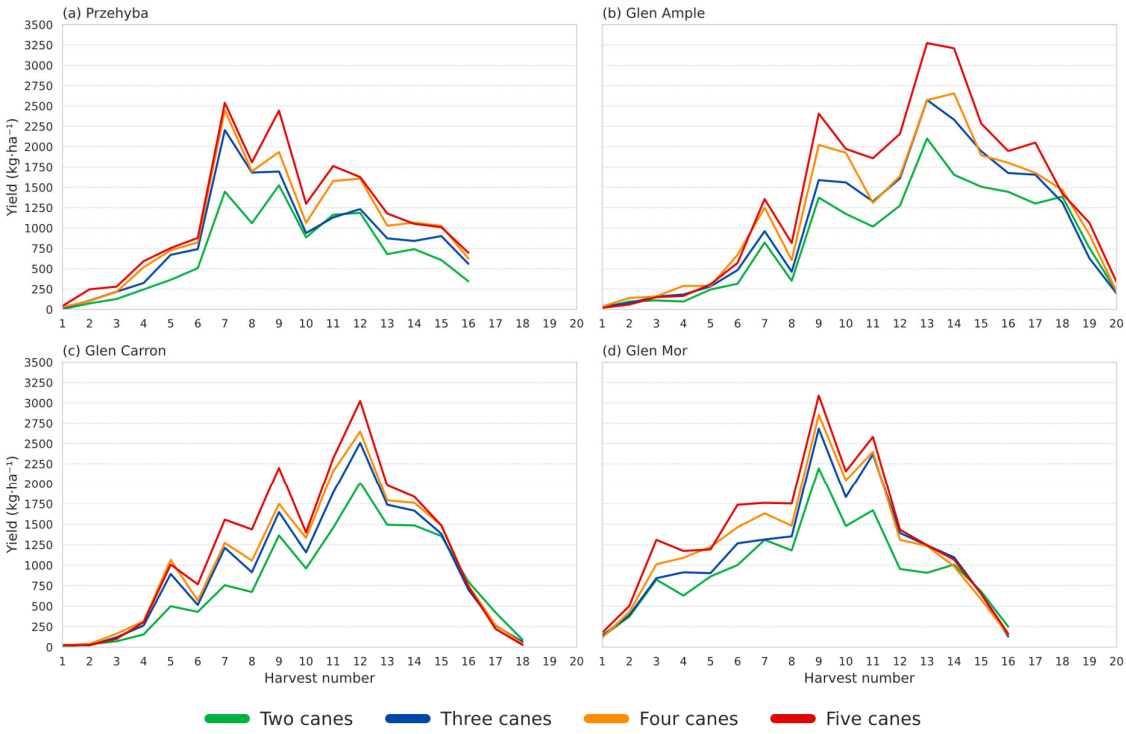

Figure 9. Yield depends on harvest: (a) Przehyba ; (b) Glen Ample; (c) Glen Carron; (d) Glen Mor.

The distribution of fruit number across successive harvest dates, as influenced by cane number and cultivar, is shown in Figure 10. Across all cultivars, the number of fruits per hectare exhibited a clearly structured temporal pattern over successive harvests. Fruit number increased during the early harvests, reached a pronounced maximum in the mid-season period, and subsequently declined towards the final harvests. This seasonal trajectory was consistent across cane-number treatments within each cultivar.

Cane number primarily affected the magnitude of fruit number rather than the timing of peak occurrence. For all cultivars, higher cane-number combinations consistently produced a greater number of fruits across most harvests, with the five-cane treatment maintaining the highest fruit counts throughout the season and the two-cane treatment remaining distinctly lower. Treatments with three and four canes generally followed intermediate trajectories between these extremes.

Temporal fluctuations in fruit number were largely synchronous across cane combinations within each cultivar. Peaks and declines occurred at similar harvests regardless of cane number, indicating that short-term variation in fruit number was driven mainly by harvest timing rather than by shifts in treatment ranking.

Fruit number dynamics revealed a stable hierarchy of cane-number treatments within each cultivar, superimposed on a common seasonal pattern of fruit production.

 doi:10.20944/preprints202604.1152.v1

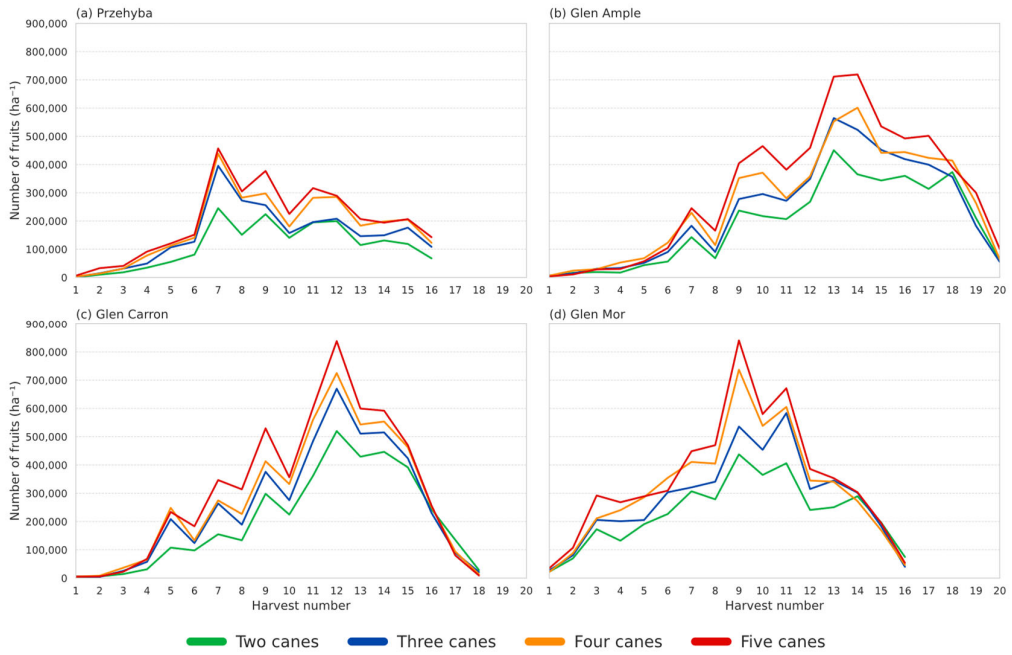

Figure 10. Number of fruits depends on harvest: (a) Przehyba ; (b) Glen Ample; (c) Glen Carron; (d) Glen Mor.

Changes in mean fruit weight across successive harvest dates, as influenced by cane number and cultivar, are shown in Figure 11. Across all cultivars, mean fruit weight exhibited a clear temporal pattern characterised by a gradual decline over successive harvests. Higher fruit weights were observed during the early harvests, followed by a progressive reduction towards the end of the harvest period.

Differences among cane number were comparatively small relative to temporal variation. Within each cultivar, trajectories corresponding to different cane-number combinations remained closely aligned throughout most of the harvest season, indicating that cane number exerted a limited effect on mean fruit weight compared with harvest timing.

Temporal fluctuations in fruit weight occurred synchronously across treatments within each cultivar. Short-term deviations were occasionally observed at individual harvests; however, these did not alter the overall similarity of trajectories among cane-number treatments. Mean fruit weight was primarily structured by harvest progression rather than by cane-number treatment, with only minor and cultivar-specific deviations between treatments.

 doi:10.20944/preprints202604.1152.v1

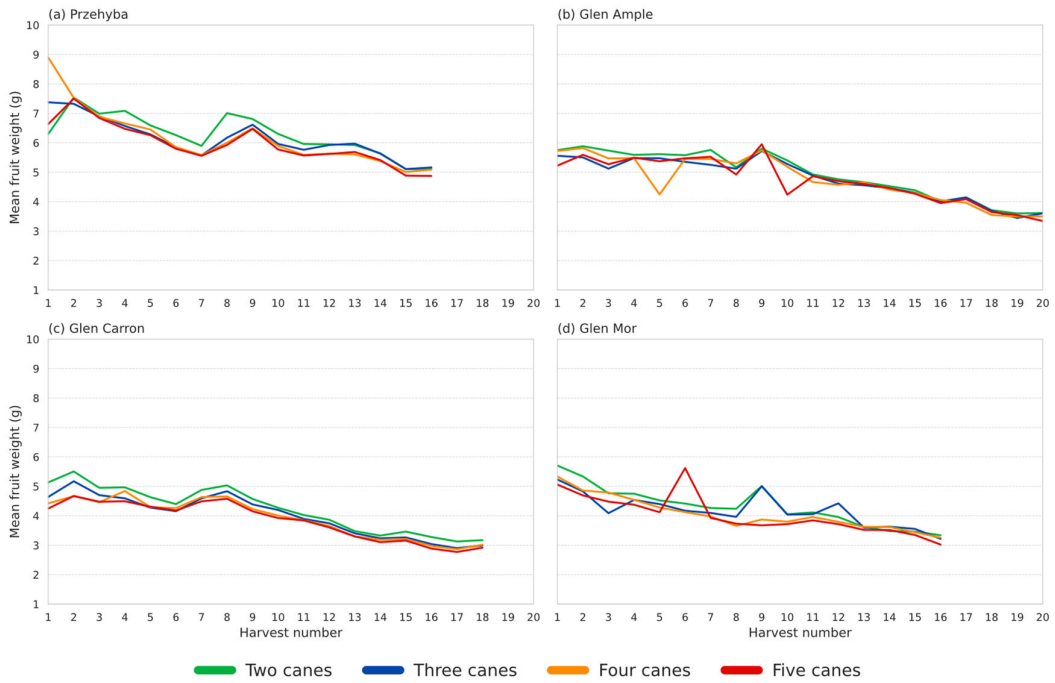

Figure 11. Mean fruit weight depends on harvest: (a) Przehyba ; (b) Glen Ample; (c) Glen Carron; (d) Glen Mor.

Across all analysed cultivars, significant differences were observed for all evaluated yield parameters, including yield per plant, fruit number per plant, and average fruit weight (Table 7).

Among the cultivars, Glen Ample was characterized by the highest yield per plant and the greatest number of fruits per plant, whereas the lowest values for both parameters were recorded in Przehyba. In contrast, average fruit weight exhibited an opposite pattern, with the highest values observed in Przehyba and the lowest in Glen Carron.

The cane-number combinations factor also significantly affected all analysed yield parameters. Yield per plant and fruit number per plant increased progressively with increasing cane number, with the highest values observed in the five-cane treatment and the lowest in the two-cane treatment. Intermediate cane numbers formed clearly separated groups, indicating a well-ordered response across treatments. In contrast, average fruit weight decreased with increasing cane number. The highest fruit weight was recorded in the two-cane treatment, whereas the lowest values were observed in the four and five canes combinations. A significant interaction between cultivar and combinations was detected for all analysed yield parameters, indicating that the magnitude of response to cane density differed among cultivars.

Table 7. Main factorial effects on yield parameters.

		Yield per plant (g)	Number of fruits per plant (pcs.)	Fruit weight (g)
Cultivar (A)	Przehyba	1868.06 d	298.47 c	6.29 a
	Glen Ample	2790.59 a	616.89 a	4.53 b
	Glen Carron	2150.17 c	580.11 b	3.71 d
	Glen Mor	2374.02 b	586.88 b	4.06 c
	p-value	< 0.001	< 0.001	< 0.001
Combination (B)	Two canes	1790.90 d	397.92 d	4.78 a
	Three canes	2200.55 c	494.23 c	4.68 b
	Four canes	2445.96 b	559.97 b	4.58 c
	Five canes	2745.43 a	630.64 a	4.56 c
	p-value	< 0.001	< 0.001	< 0.001

 doi:10.20944/preprints202604.1152.v1

A*B	*p*-value	0.004	0.001	0.012

3.2. Vegetation Indices

Temporal dynamics of vegetation indices for Przehyba cultivar revealed consistent patterns across cane-number treatments, although the magnitude and differentiation among treatments varied depending on the index (Figure 12).

For GNDVI, all treatments exhibited a similar temporal pattern, characterized by an increase from the initial measurements to a peak around the third measurement, followed by a gradual decline and a subsequent increase at the final measurement. Differences among cane-number treatments were relatively small throughout the season, indicating limited sensitivity of this index to cane density.

A comparable temporal trend was observed for NDRE, with values increasing during the early measurements, followed by moderate fluctuations and a final increase at the end of the measurement period. Treatment-related differences were more pronounced than for GNDVI, particularly in the later measurements, although no consistent ranking of treatments across all time points was observed.

OSAVI showed a similar dynamic pattern, with a clear increase up to the third measurement and subsequent fluctuations. Differences among treatments were generally small, with occasional divergence at specific time points, but without a stable and consistent separation among cane-number treatments.

In contrast, MCARI2 exhibited greater variability across both time and treatments. While a general increase was observed during the early measurements, followed by fluctuations in later stages, this index showed more pronounced differences among cane-number treatments at selected time points. However, as with the other indices, no consistent treatment ranking was maintained throughout the entire measurement period.

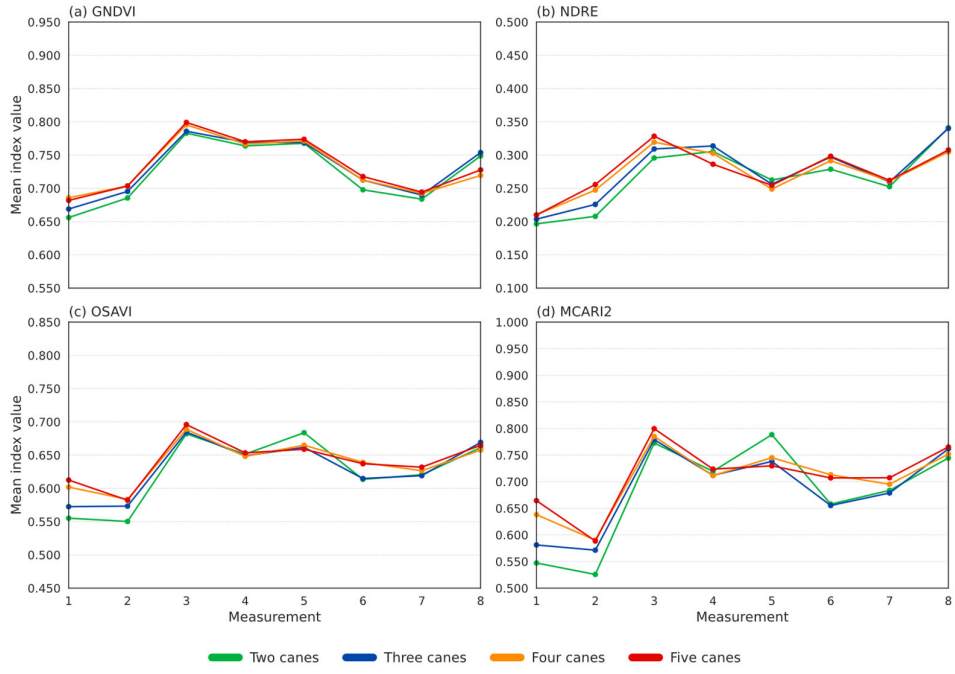

Figure 12. Mean index value depending on measurement for the Przehyba cultivar: (a) GNDVI; (b) NDRE; (c) OSAVI; (d) MCARI2.

 doi:10.20944/preprints202604.1152.v1

Temporal dynamics of vegetation indices in the cultivar Glen Ample showed consistent seasonal patterns across all cane-number treatments, with relatively limited differentiation among treatments (Figure 13).

For GNDVI, all treatments followed a similar temporal trajectory, with a marked increase from the initial measurements to a peak around the third measurement, followed by moderate fluctuations and a slight increase at the end of the measurement period. Differences among cane-number treatments were minor throughout the season, indicating low sensitivity of this index to cane density.

NDRE exhibited a comparable pattern, with values increasing during the early measurements and showing moderate variability in the later stages. Treatment-related differences were slightly more pronounced than for GNDVI, particularly in the final measurement, where higher values were observed for the lower cane-density treatments. However, no consistent ranking of treatments was maintained across all time points.

OSAVI followed a similar temporal trend, with an initial increase and subsequent fluctuations throughout the season. Differences among treatments were generally small, with occasional divergence at specific measurements, but without a stable separation among cane-number treatments.

In contrast, MCARI2 displayed greater variability both over time and among treatments. While a general increase was observed in the early measurements, followed by fluctuations, more distinct differences among cane-number treatments appeared at selected time points, particularly around the fifth measurement. Nevertheless, these differences were not consistent across the entire measurement period.

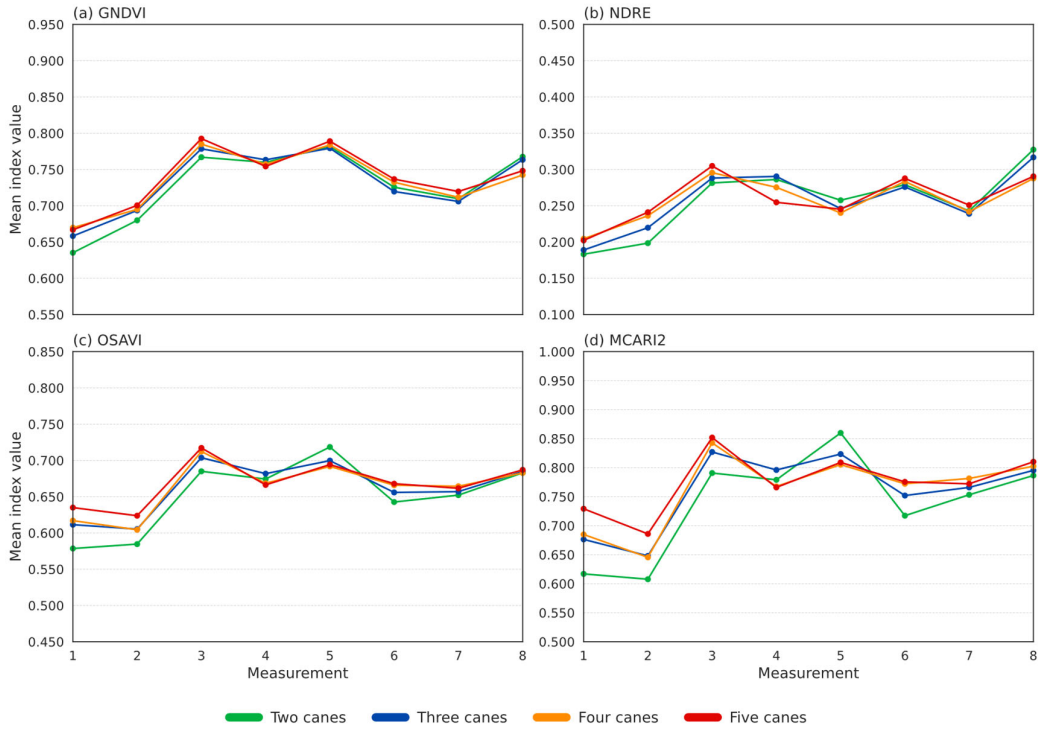

Figure 13. Mean index value depending on measurement for the Glen Ample cultivar: (a) GNDVI; (b) NDRE; (c) OSAVI; (d) MCARI2.

Temporal dynamics of vegetation indices in the cultivar Glen Carron followed consistent seasonal patterns across all cane-number treatments, with generally limited and non-uniform differentiation among treatments (Figure 14).

 doi:10.20944/preprints202604.1152.v1

For GNDVI, all treatments exhibited a similar temporal trajectory, with a pronounced increase from the initial measurements to a peak around the third measurement, followed by gradual fluctuations and a final increase at the end of the measurement period. Differences among cane-number treatments were small and did not show a stable pattern over time.

NDRE displayed a comparable dynamic, with an increase during the early measurements and moderate variability in later stages. While some differences among treatments were observed at individual time points, particularly in the early measurements, no consistent ranking of cane-number treatments was maintained throughout the season.

OSAVI followed a similar temporal pattern, characterized by an increase up to the third measurement and subsequent fluctuations. Differences among treatments were generally minor, with only slight divergence at selected time points and without a consistent separation among cane-number treatments.

MCARI2 exhibited greater variability compared with the other indices, both over time and among treatments. A clear increase was observed during the early measurements, followed by fluctuations in later stages. More pronounced differences among treatments appeared at selected time points, particularly in the early measurements, where higher values were observed in treatments with a greater number of canes. However, these differences were not maintained consistently across the entire measurement period.

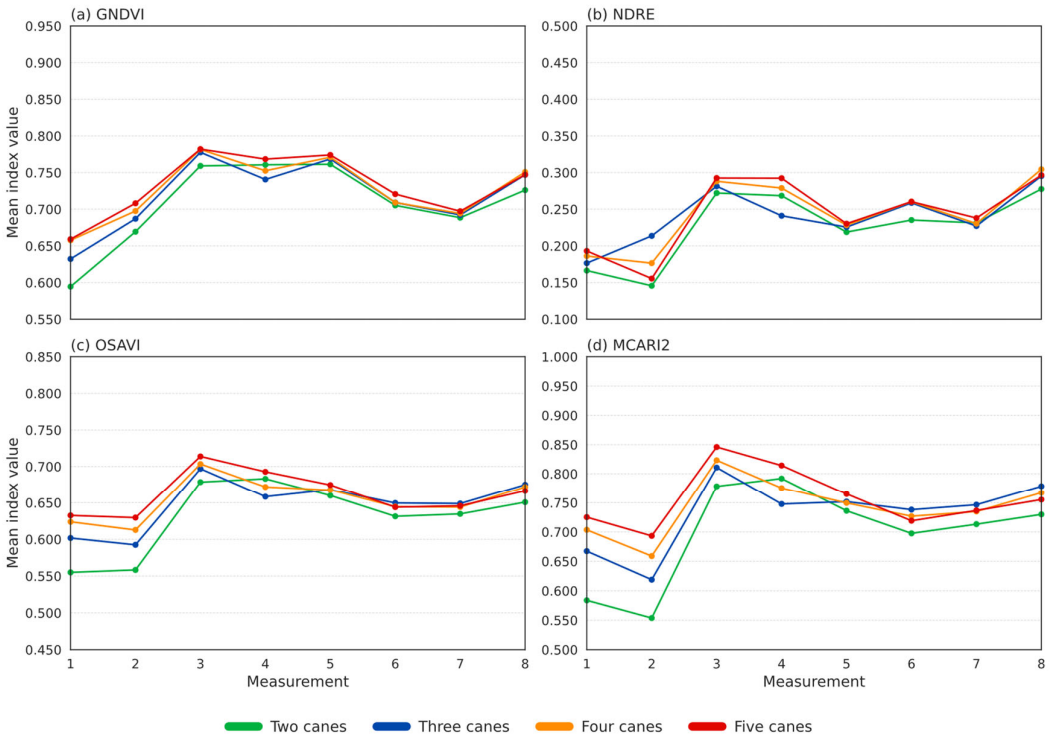

Figure 14. Mean index value depending on measurement for the Glen Carron cultivar: (a) GNDVI; (b) NDRE; (c) OSAVI; (d) MCARI2.

Temporal dynamics of vegetation indices in the cultivar Glen Mor exhibited clear seasonal patterns, with moderate and index-dependent differentiation among cane-number treatments (Figure 15).

For GNDVI, all treatments followed a similar temporal trajectory, characterized by an increase from the initial measurements to a peak around the third measurement, followed by a gradual decline and partial recovery toward the end of the season. Differences among cane-number treatments were relatively small, although slightly higher values were generally observed in treatments with a greater number of canes at selected time points.

 doi:10.20944/preprints202604.1152.v1

NDRE showed a comparable pattern, with a marked increase in the early measurements and subsequent fluctuations. Differences among treatments were more pronounced than for GNDVI, particularly in the later measurements, where higher values were often recorded in the four- and five-cane treatments. However, these differences were not entirely consistent across all measurement dates.

OSAVI exhibited a similar temporal pattern, with a clear increase up to the third measurement followed by gradual variation. Differences among treatments remained moderate, with a tendency for slightly higher values in treatments with higher cane numbers, although without a stable separation across the entire measurement period.

MCARI2 displayed the greatest variability among indices, both over time and among treatments. A pronounced increase was observed during the early measurements, followed by fluctuations in later stages. Clear differentiation among cane-number treatments was observed at several time points, with higher values generally associated with three- and four-cane treatments, while the two-cane treatment consistently exhibited lower values.

Overall, vegetation index dynamics in Glen Mor were primarily driven by seasonal canopy development, while the effect of cane number was secondary and varied depending on the specific index and measurement date.

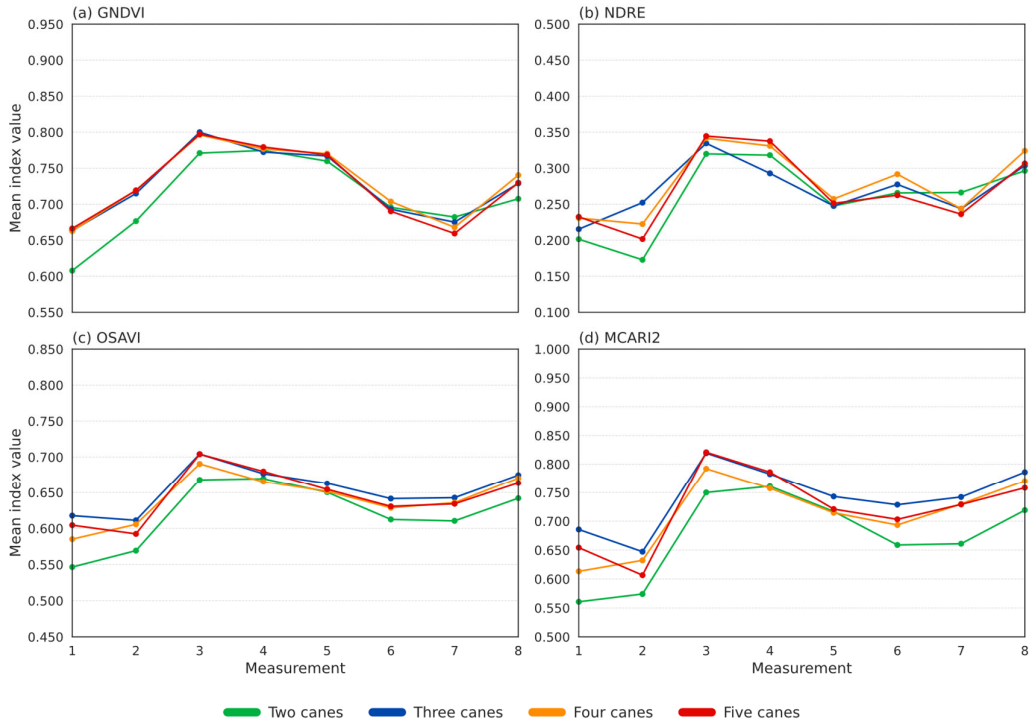

Figure 15. Mean index value depending on measurement for the Glen Mor cultivar: (a) GNDVI; (b) NDRE; (c) OSAVI; (d) MCARI2.

The analysis of vegetation indices for the Przehyba cultivar is presented in Table 8. For the Przehyba cultivar, mean vegetation index values exhibited index-dependent responses to cane-number treatments. For GNDVI, MCARI2, and OSAVI, mean index values decreased with decreasing cane number, indicating lower average index levels under reduced cane density. In contrast, NDRE did not show a clear monotonic response across cane-number treatments; however, the two-cane combination was consistently characterised by lower mean index values relative to the remaining treatments.

The mean coefficient of variation, showed contrasting responses among vegetation indices. For GNDVI, MCARI2, and OSAVI, the coefficient of variation decreased with increasing cane density,

 doi:10.20944/preprints202604.1152.v1

indicating progressively more spatially uniform canopy signals under denser configurations. In contrast, NDRE exhibited an opposite pattern, with mean coefficient of variation increasing as cane number increased, reflecting greater spatial heterogeneity at higher cane densities for this index.

The total amplitude of vegetation index dynamics exhibited index-specific responses to cane density. For GNDVI, no clear monotonic trend with cane number was observed. the lowest total amplitude occurred for the four cane combination, while the highest amplitude was associated with the two cane. A similarly non-monotonic pattern was evident for NDRE, with the lowest amplitude recorded for the two cane combination and the highest for the three-cane treatment. In contrast, MCARI2 showed a clear density-related gradient, with total amplitude increasing as cane density decreased, indicating progressively larger cumulative temporal changes under lower-density configurations. For OSAVI, the two-cane combination displayed a distinctly higher total amplitude compared with the remaining treatments, which clustered at similar, lower levels.

The total relative amplitude of vegetation index dynamics showed patterns largely consistent with those observed for absolute amplitude. For GNDVI and OSAVI, relative amplitude did not exhibit a clear monotonic response to cane density, with the highest values generally associated with the lowest-density treatment and more similar values across the remaining combinations. MCARI2 again displayed a distinct density-related response, with higher relative amplitudes under lower cane densities and a progressive attenuation as cane number increased. NDRE deviated from this general pattern. The lowest relative amplitude values were observed for the two- and four-cane combinations, whereas the three-cane treatment showed a clearly higher relative amplitude, indicating a non-monotonic and less density-ordered response for this index.

The total relative increase component of vegetation index dynamics exhibited index-specific and largely non-monotonic responses to cane density. For GNDVI, the highest relative increases were observed for the four- and five-cane combinations, while the lowest values occurred for the three-cane treatment, resulting in no clear density-dependent trend. A similarly non-monotonic pattern was observed for MCARI2, with the smallest relative increase associated with the three-cane combination and the largest values recorded for the two-cane treatment. In contrast, NDRE showed a clear and consistent density-related response, with relative increases progressively rising with increasing cane number. OSAVI did not display a monotonic pattern, the lowest relative increase was observed for the three cane combination, whereas higher values were recorded for the two, four, and five cane combinations.

The total relative decrease component showed clear index-specific responses to cane density. For MCARI2, a distinct density-related trend was observed, with progressively lower relative decrease values associated with higher cane densities. NDRE did not exhibit a consistent pattern; the lowest relative decrease occurred for the four-cane combination, while the highest value was recorded for the three-cane treatment. For GNDVI and OSAVI, relative decrease values formed two clearly separated groups rather than a monotonic gradient. Higher values were generally associated with the two- and three-cane combinations, whereas lower values characterised the four- and five-cane treatments, indicating a stepwise rather than continuous response to increasing cane density.

Temporal roughness exhibited distinct index-specific patterns in relation to cane density. For GNDVI and OSAVI, no clear monotonic trend was observed; however, the two-cane combination consistently showed the highest roughness values, while the remaining cane-density treatments were characterised by more similar and closely grouped roughness levels. In contrast, MCARI2 displayed a clear density-dependent response, with roughness decreasing progressively as cane density increased, indicating smoother temporal dynamics under higher-density configurations. NDRE did not follow a consistent density-related pattern, with the lowest roughness recorded for the five-cane combination and the highest value observed for the three-cane treatment.

Table 8. Vegetation indices of the Przehyba cultivar.

 doi:10.20944/preprints202604.1152.v1

VI	Combination Przehyba	VI mean	CV mean	VI total A	VI A total relative (%)	VI A increase relative (%)	VI A decrease relative (%)	VI roughness dynamics
GNDVI	Two canes	0.723	0.090	0.299	0.423	0.136	0.287	0.417
GNDVI	Three canes	0.730	0.089	0.277	0.389	0.127	0.262	0.363
GNDVI	Four canes	0.731	0.086	0.249	0.342	0.141	0.201	0.377
GNDVI	Five canes	0.733	0.088	0.263	0.362	0.141	0.220	0.381
MCARI2	Two canes	0.680	0.166	0.608	0.967	0.274	0.694	1.081
MCARI2	Three canes	0.685	0.167	0.500	0.773	0.215	0.558	0.860
MCARI2	Four canes	0.704	0.160	0.456	0.696	0.237	0.459	0.773
MCARI2	Five canes	0.711	0.156	0.450	0.690	0.241	0.450	0.766
NDRE	Two canes	0.267	0.199	0.283	1.160	0.235	0.925	0.424
NDRE	Three canes	0.276	0.201	0.327	1.273	0.310	0.963	0.497
NDRE	Four canes	0.273	0.205	0.297	1.143	0.335	0.808	0.405
NDRE	Five canes	0.275	0.206	0.318	1.208	0.361	0.848	0.389
OSAVI	Two canes	0.627	0.095	0.317	0.522	0.156	0.366	0.575
OSAVI	Three canes	0.631	0.093	0.262	0.426	0.123	0.303	0.462
OSAVI	Four canes	0.639	0.088	0.251	0.405	0.148	0.256	0.427
OSAVI	Five canes	0.642	0.086	0.252	0.408	0.152	0.256	0.430

* Vegetation index (VI); Mean vegetation index (VI mean); Mean coefficient of variation vegetation index (CV mean); Total amplitude of vegetation index (VI Total A); Total relative vegetation index amplitude (%) (VI A Total relative (%)); Total relative increase change of vegetation index amplitude (%) (VI A Increase relative (%)); Total relative decrease change of vegetation index amplitude (%) (VI A decrease relative (%)); Roughness of vegetation index dynamics (VI Roughness dynamics).

The analysis of vegetation indices for the Glen Ample cultivar is presented in Table 9. For the Glen Ample cultivar, mean vegetation index values showed index-dependent responses to cane density. For GNDVI, MCARI2, and OSAVI, a clear and monotonic increasing trend was observed, with mean index values progressively rising as the number of canes per plant increased. The lowest VI mean values were consistently associated with the two-cane combination, whereas the highest values occurred under the five-cane treatment, with no deviations from this density-related gradient. In contrast, NDRE did not exhibit a distinct density-dependent trend. Mean NDRE values remained very similar across all cane-number combinations, and the observed differences were small and did not form an ordered pattern with increasing cane density. Consequently, NDRE showed the lowest sensitivity of mean index values to changes in cane density among the analysed vegetation indices.

The mean coefficient of variation of vegetation indices exhibited a clear density-related pattern for GNDVI, MCARI2, and OSAVI. For these indices, higher CV mean values were consistently associated with lower cane densities, indicating increased spatial variability under sparser canopy configurations. As cane number increased, CV mean values progressively decreased, forming a coherent and monotonic gradient across the analysed cane-density treatments. In contrast, NDRE did not show a consistent monotonic response to cane density. Although CV mean values varied only moderately across most cane-number combinations, the highest spatial variability was distinctly

 doi:10.20944/preprints202604.1152.v1

associated with the five-cane treatment, separating this combination from the remaining density levels. As a result, NDRE displayed a non-uniform and less density-ordered pattern of spatial variability compared with the other vegetation indices.

The total amplitude of vegetation index dynamics did not exhibit a clear or monotonic response to cane density for any of the analysed indices. Instead, index-specific and non-uniform patterns were observed across cane-number treatments. For GNDVI, the highest total amplitude was recorded for the five-cane combination, whereas the lowest value occurred under the four-cane treatment, with intermediate densities showing no ordered progression. In the case of MCARI2, the largest total amplitude was clearly associated with the two-cane combination, while the three-, four-, and five-cane treatments displayed distinctly lower and relatively similar amplitude values, indicating a marked separation between the lowest-density treatment and the remaining combinations. For NDRE, the greatest total amplitude was observed for the three-cane combination, whereas the lowest values occurred for the two- and four-cane treatments, resulting in a non-monotonic and irregular distribution across cane densities. A comparable absence of a density-driven gradient was evident for OSAVI, for which the highest total amplitude was associated with the two-cane combination and the lowest value was recorded for the three-cane treatment, with the remaining combinations occupying intermediate positions.

The total relative amplitude of vegetation index dynamics also did not show a clear or monotonic dependence on cane density for any of the analysed indices. Instead, index-specific and non-linear response patterns were observed across cane-number treatments. For GNDVI, the highest relative amplitude was associated with the two-cane combination, whereas the lowest value occurred under the four-cane treatment, with the remaining combinations occupying intermediate positions. A similar structure was observed for MCARI2, for which the greatest relative amplitude was again recorded for the two-cane combination, while the three-, four-, and five-cane treatments exhibited distinctly lower and comparatively similar values, indicating a clear separation between the lowest-density treatment and the remaining cane-number classes. For NDRE, the highest relative amplitude was observed for the three-cane combination, whereas the lowest value was associated with the five-cane treatment, resulting in a non-monotonic and irregular pattern across cane densities. In the case of OSAVI, the largest relative amplitude occurred under the two-cane configuration, while the smallest value was recorded for the three-cane combination, with no consistent density-related gradient evident across the remaining treatments.

The total relative increase component of vegetation index exhibited index-specific responses to cane density, ranging from clear density-driven trends to non-monotonic patterns. For GNDVI, a distinct and coherent increasing trend was observed, with relative increase values rising progressively as cane density increased. Lower-density combinations were characterised by smaller cumulative relative increases, whereas higher cane-number treatments consistently showed larger values, forming a clear density-related gradient. A similar, although less pronounced, pattern was observed for NDRE. While the increase in relative values was not strictly monotonic, higher cane-density treatments were generally associated with larger relative increases compared with the two-cane combination, which consistently exhibited the lowest values. This indicates a moderate positive association between cane density and cumulative relative increases for NDRE. In contrast, MCARI2 displayed a non-monotonic response. The lowest relative increase was recorded for the three-cane combination, whereas the highest values occurred under both the two- and five-cane treatments, resulting in a U-shaped pattern rather than a density-ordered gradient. For OSAVI, relative increase values were clearly differentiated across cane-number treatments, with the smallest value observed for the three-cane combination and the highest value associated with the five-cane treatment, indicating a strong separation between intermediate and high-density configurations.

The total relative decrease component of vegetation index showed clear but index-specific responses to cane density, with strong contrasts between low- and high-density treatments. For GNDVI, the highest relative decrease was distinctly associated with the two-cane combination, whereas the lowest value occurred under the four-cane treatment, indicating a pronounced reduction

 doi:10.20944/preprints202604.1152.v1

in cumulative negative changes with increasing cane density. A comparable but more strongly differentiated pattern was observed for MCARI2, for which the two-cane treatment exhibited clearly the highest relative decrease, while the remaining cane-number combinations were characterised by substantially lower and relatively similar values. For NDRE, relative decrease values formed two clearly separated groups. The two and three cane combinations showed the highest cumulative relative decreases, whereas markedly lower values were associated with the four- and five-cane treatments, indicating a stepwise rather than continuous response to increasing cane density. An analogous pattern was observed for OSAVI, which followed the same structure as MCARI2, with the highest relative decrease occurring under the two-cane configuration and distinctly lower values recorded for all higher-density treatments.

The roughness of vegetation index dynamics exhibited clear but index-specific responses to cane density, ranging from monotonic trends to strongly non-linear patterns. For GNDVI, a distinct increasing trend was observed, with temporal roughness values rising progressively as cane density increased. Lower-density treatments were characterised by smoother temporal trajectories, whereas higher cane-number combinations exhibited increased roughness, forming a clear density-related gradient. In contrast, MCARI2 showed an inverse density-related response, with the highest roughness clearly associated with the two-cane combination, while substantially lower values were recorded for the higher-density treatments. This indicates markedly smoother temporal dynamics under denser cane configurations for this index. For NDRE, roughness values formed two clearly separated groups. The two- and three-cane combinations exhibited the highest roughness values, whereas the four- and five-cane treatments were characterised by distinctly lower roughness, indicating a stepwise rather than continuous response to increasing cane density. A similar non-monotonic structure was observed for OSAVI, for which the lowest roughness value occurred under the three-cane combination, while the highest roughness was associated with the two-cane treatment, with the remaining combinations occupying intermediate positions.

Table 9. Vegetation indices of the Glen Ample cultivar.

VI	Combination Glen Ample	VI mean	CV mean	VI total A	VI A total relative (%)	VI A increase relative (%)	VI A decrease relative (%)	VI roughness dynamics
GNDVI	Two canes	0.728	0.094	0.291	0.412	0.103	0.309	0.358
GNDVI	Three canes	0.733	0.089	0.282	0.394	0.115	0.278	0.374
GNDVI	Four canes	0.735	0.086	0.272	0.375	0.129	0.245	0.396
GNDVI	Five canes	0.738	0.082	0.297	0.405	0.138	0.268	0.429
MCARI2	Two canes	0.739	0.178	0.497	0.695	0.196	0.499	0.884
MCARI2	Three canes	0.760	0.157	0.381	0.534	0.166	0.368	0.676

 doi:10.20944/preprints202604.1152.v1

MCARI2	Four canes	0.763	0.158	0.412	0.581	0.188	0.393	0.746
MCARI2	Five canes	0.775	0.145	0.413	0.553	0.206	0.347	0.738
NDRE	Two canes	0.257	0.226	0.274	1.179	0.229	0.950	0.407
NDRE	Three canes	0.258	0.223	0.290	1.216	0.287	0.929	0.406
NDRE	Four canes	0.258	0.221	0.278	1.121	0.344	0.777	0.374
NDRE	Five canes	0.260	0.231	0.281	1.118	0.330	0.788	0.387
OSAVI	Two canes	0.652	0.105	0.277	0.431	0.121	0.310	0.487
OSAVI	Three canes	0.662	0.091	0.217	0.337	0.104	0.233	0.398
OSAVI	Four canes	0.663	0.090	0.233	0.362	0.122	0.241	0.433
OSAVI	Five canes	0.669	0.081	0.242	0.366	0.136	0.230	0.434

* Vegetation index (VI); Mean vegetation index (VI mean); Mean coefficient of variation vegetation index (CV mean); Total amplitude of vegetation index (VI Total A); Total relative vegetation index amplitude (%) (VI A Total relative (%)); Total relative increase change of vegetation index amplitude (%) (VI A Increase relative (%)); Total relative decrease change of vegetation index amplitude (%) (VI A decrease relative (%)); Roughness of vegetation index dynamics (VI Roughness dynamics).

The analysis of vegetation indices for the Glen Carron cultivar is presented in Table 10. For the Glen Carron cultivar, mean vegetation index values showed a clear and consistent response to cane density across all analysed indices. For GNDVI, MCARI2, NDRE, and OSAVI, mean values increased progressively with increasing cane number, forming a distinct and monotonic gradient from the two-cane to the five-cane treatment. The lowest values were consistently associated with the two-cane combination, whereas the highest values occurred under the five-cane configuration.

The mean coefficient of variation of vegetation indices also exhibited a relatively clear density-related pattern. For all indices, the highest values were observed under the two-cane treatment, indicating greater spatial variability under lower cane density. As cane number increased, values decreased, with the lowest variability generally recorded for the higher-density treatments. This pattern reflects increasing spatial uniformity of canopy structure with increasing cane density.

The total amplitude of vegetation index dynamics showed a more index-specific response. A clear density-related trend was observed only for NDRE, for which amplitude values increased progressively with increasing cane number, from the lowest value in the two-cane treatment to the highest value in the five-cane configuration. In contrast, GNDVI, MCARI2, and OSAVI did not exhibit a consistent monotonic response to cane density, with amplitude values varying among treatments without forming a clear density-dependent gradient.

The total relative amplitude of vegetation index dynamics exhibited index-specific responses to cane density. A clear and consistent decreasing trend with increasing cane number was observed for

 doi:10.20944/preprints202604.1152.v1

MCARI2 and OSAVI, with the highest relative amplitude values associated with the two-cane treatment and progressively lower values under higher cane densities.

The total relative increase component showed a clear density-dependent pattern only for OSAVI. For this index, relative increase values rose progressively with increasing cane number, indicating greater cumulative positive dynamics under higher-density configurations. For the remaining indices, no consistent trend was observed.

The total relative decrease component exhibited a clear density-related response for MCARI2 and OSAVI. For both indices, relative decrease values declined with increasing cane number, with the highest values recorded for the two-cane treatment and lower values observed under higher-density configurations.

Temporal roughness did not exhibit a clear or consistent response to cane density for any of the analysed vegetation indices.

Table 10. Vegetation indices of the Glen Carron cultivar.

VI	Combination Glen Carron	VI mean	CV mean	VI total A	VI A total relative (%)	VI A increase relative (%)	VI A decrease relative (%)	VI roughness dynamics
GNDVI	Two canes	0.708	0.092	0.277	0.415	0.097	0.318	0.254
GNDVI	Three canes	0.719	0.086	0.342	0.484	0.149	0.336	0.430
GNDVI	Four canes	0.727	0.081	0.305	0.425	0.138	0.287	0.404
GNDVI	Five canes	0.732	0.078	0.269	0.376	0.119	0.258	0.294
MCARI2	Two canes	0.698	0.184	0.395	0.643	0.174	0.469	0.608
MCARI2	Three canes	0.732	0.158	0.362	0.539	0.169	0.370	0.626
MCARI2	Four canes	0.742	0.158	0.345	0.489	0.185	0.304	0.501
MCARI2	Five canes	0.757	0.144	0.348	0.472	0.202	0.270	0.454
NDRE	Two canes	0.227	0.239	0.267	1.483	0.340	1.144	0.460
NDRE	Three canes	0.240	0.222	0.293	1.303	0.329	0.974	0.376
NDRE	Four canes	0.244	0.218	0.317	1.475	0.381	1.094	0.532
NDRE	Five canes	0.245	0.219	0.348	1.753	0.494	1.259	0.599

 doi:10.20944/preprints202604.1152.v1

OSAVI	Two canes	0.631	0.108	0.199	0.336	0.077	0.259	0.310
OSAVI	Three canes	0.649	0.090	0.207	0.331	0.099	0.231	0.378
OSAVI	Four canes	0.655	0.090	0.189	0.296	0.105	0.191	0.321
OSAVI	Five canes	0.662	0.083	0.180	0.275	0.106	0.169	0.260

* Vegetation index (VI); Mean vegetation index (VI mean); Mean coefficient of variation vegetation index (CV mean); Total amplitude of vegetation index (VI Total A); Total relative vegetation index amplitude (%) (VI A Total relative (%)); Total relative increase change of vegetation index amplitude (%) (VI A Increase relative (%)); Total relative decrease change of vegetation index amplitude (%) (VI A decrease relative (%)); Roughness of vegetation index dynamics (VI Roughness dynamics).

The analysis of vegetation indices for the Glen Mor cultivar is presented in Table 11. For the Glen Mor cultivar, mean vegetation index values did not exhibit a clear or consistent response to cane density for any of the analysed indices. Although slight variations were observed among cane-number treatments, these differences did not form a monotonic or well-ordered pattern for GNDVI, MCARI2, NDRE, or OSAVI.

A similar lack of a clear density-related pattern was observed for the mean coefficient of variation of vegetation indices. CV mean values varied across cane-number treatments, but no consistent trend was detected for any of the indices, indicating comparable levels of spatial variability across the analysed density configurations.

The total amplitude of vegetation index dynamics exhibited index-specific responses to cane density. A clear and consistent increasing trend was observed for GNDVI and NDRE, with amplitude values rising progressively with increasing cane number, indicating greater cumulative temporal variability under higher-density configurations. In contrast, MCARI2 and OSAVI did not show a consistent or monotonic response.

The total relative amplitude of vegetation index dynamics showed a clear density-dependent pattern only for GNDVI. For this index, relative amplitude increased progressively with increasing cane number. In contrast, MCARI2, NDRE, and OSAVI did not exhibit a consistent response to cane density.

The total relative increase component displayed a clear density-related trend for GNDVI and NDRE, with relative increase values rising as cane number increased. This indicates greater cumulative positive dynamics under higher-density conditions for these indices. For MCARI2 and OSAVI, no consistent trend was observed.

The total relative decrease component did not show a clear or consistent response to cane density for any of the analysed indices. Values varied across treatments without forming a monotonic or structured pattern.

Temporal roughness also did not exhibit a clear density-related trend. Roughness values differed among cane-number treatments but did not follow a consistent or ordered pattern for any vegetation index.

Table 11. Vegetation indices of the Glen Mor cultivar.

VI	Combination Glen Mor	VI mean	CV mean	VI total A	VI A total relative (%)	VI A increase relative (%)	VI A decrease relative (%)	VI roughness dynamics

 doi:10.20944/preprints202604.1152.v1

GNDVI	Two canes	0.709	0.102	0.285	0.418	0.123	0.295	0.274
GNDVI	Three canes	0.727	0.083	0.315	0.440	0.164	0.276	0.365
GNDVI	Four canes	0.730	0.088	0.334	0.471	0.170	0.301	0.328
GNDVI	Five canes	0.726	0.084	0.339	0.477	0.183	0.295	0.345
MCARI2	Two canes	0.675	0.196	0.362	0.575	0.139	0.436	0.512
MCARI2	Three canes	0.742	0.147	0.358	0.514	0.171	0.343	0.506
MCARI2	Four canes	0.713	0.162	0.354	0.522	0.130	0.392	0.426
MCARI2	Five canes	0.722	0.159	0.434	0.652	0.223	0.430	0.635
NDRE	Two canes	0.261	0.198	0.297	1.409	0.369	1.040	0.529
NDRE	Three canes	0.271	0.192	0.330	1.264	0.401	0.864	0.405
NDRE	Four canes	0.280	0.199	0.374	1.453	0.454	0.999	0.639
NDRE	Five canes	0.272	0.197	0.375	1.560	0.509	1.051	0.635
OSAVI	Two canes	0.621	0.116	0.214	0.359	0.090	0.269	0.282
OSAVI	Three canes	0.654	0.083	0.195	0.306	0.102	0.204	0.295
OSAVI	Four canes	0.642	0.090	0.209	0.333	0.092	0.241	0.252
OSAVI	Five canes	0.645	0.089	0.230	0.368	0.128	0.240	0.316

* Vegetation index (VI); Mean vegetation index (VI mean); Mean coefficient of variation vegetation index (CV mean); Total amplitude of vegetation index (VI Total A); Total relative vegetation index amplitude (%) (VI A Total relative (%)); Total relative increase change of vegetation index amplitude (%) (VI A Increase relative (%)); Total relative decrease change of vegetation index amplitude (%) (VI A decrease relative (%)); Roughness of vegetation index dynamics (VI Roughness dynamics).

4. Discussion

The present study investigated the effect of cane density on yield in floricane raspberry cultivars, with the integration of multispectral imaging acquired using an unmanned aerial vehicle. Although

 doi:10.20944/preprints202604.1152.v1

cane density has been widely studied in raspberry production, previous research has rarely incorporated remote sensing approaches for quantitative analysis.

Cane density exerted a strong and consistent effect on yield formation across all analysed cultivars. Yield per plant and fruit number per plant increased progressively with increasing cane number, indicating a clear and well-ordered response to density. In contrast, yield per cane decreased with increasing cane number, revealing a trade-off between individual cane productivity and total yield at the plant and area levels. The increase in yield was primarily driven by changes in fruit number rather than fruit size. Mean fruit weight showed limited sensitivity to cane density and exhibited cultivar-specific responses, remaining stable in some cultivars while slightly decreasing under higher densities in others.

At the plantation scale, yield per hectare increased monotonically with cane number, confirming that higher cane densities enhance overall productivity despite reduced yield per cane. This compensatory mechanism resulted in a stable hierarchy of treatments, with the highest yields consistently associated with the highest cane density.

Temporal dynamics of yield and fruit number followed a common seasonal pattern across all cultivars and cane-number treatments, characterized by an early increase, a mid-season peak, and a gradual decline. Cane density influenced the magnitude of yield and fruit number but did not alter the timing of peak production, indicating that seasonal dynamics were primarily governed by harvest progression rather than canopy density. In contrast, mean fruit weight was predominantly determined by harvest timing, showing a consistent decline over successive harvests, with only minor differences among cane-number treatments. Overall, yield formation in primocane raspberry was strongly regulated by a density-driven increase in fruit number, while fruit size remained comparatively stable and was mainly influenced by seasonal factors rather than cane density.

The influence of cane density on raspberry yield parameters was also confirmed in studies on cultivars Polonez and Enrosadira [21], Autumn Bliss [23], Polana and Polka [24], Prelude and Killarney [6], Glen Ample [25]. Moreover, the influence of treatments consisting in regulating the number of buds on yield parameters was confirmed [26]. The combined regulation of cane density and bud number can therefore be considered an integrated agronomic approach to the effective management of floricane raspberry canopies.

Management practices that directly modify shrub architecture influence not only final yield parameters but also determine the spatial organization of the canopy throughout the growing season. These changes include variations in canopy closure, vertical and horizontal biomass distribution, the balance between vegetative and generative structures, and the internal light environment within the hedgerow. As a result, cane density affects not only physiological processes at the level of individual canes but also the overall functional properties of the plant and the plantation treated as an integrated system. The resulting canopy structure generates optical signals related to chlorophyll content, soil coverage, vegetation uniformity, and temporal growth patterns. This suggests that the effects of agronomic practices, such as cane density regulation, can be assessed not only through conventional destructive measurements or visual evaluation but also through quantifiable spectral responses obtained using remote sensing techniques.

Vegetation index dynamics across all cultivars were primarily driven by seasonal canopy development rather than by cane density. All indices exhibited a consistent temporal pattern characterized by an early increase, a mid-season peak, and subsequent stabilization or decline, indicating a shared phenological trajectory across treatments. The effect of cane density on vegetation index values was generally moderate and not always consistent, with responses varying depending on the index and cultivar. In some cases, higher cane density was associated with increased index values, whereas in others the response was weak or non-monotonic. Spatial variability of vegetation indices tended to decrease with increasing cane density, suggesting more uniform canopy structure under denser configurations, although this pattern was not consistent across all cases. Metrics describing temporal dynamics revealed variable and index-dependent responses to cane density, without a uniform pattern across indices. The observed variation in vegetation index values, together

 doi:10.20944/preprints202604.1152.v1

with their spatial heterogeneity and temporal dynamics, indicates that plant responses to cane density are complex and multidimensional. A comprehensive interpretation therefore requires consideration of both spatial scale and seasonal changes. Such complexity cannot be fully captured using point-based or destructive field measurements, which do not allow simultaneous assessment of canopy uniformity, spatial structure, and temporal growth patterns. In this context, approaches that enable systematic, objective, and repeatable acquisition of phenotypic data at high spatial and temporal resolution are of particular importance.

The use of multispectral imaging in primocane raspberry cultivars allowed the identification of both spatial and temporal variability, indicating that cane density regulation is reflected not only in conventional yield and growth metrics but also in the differentiation of vegetation index values, their spatial distribution, and seasonal patterns [21].

Monitoring systems based on sensor technologies, combined with advanced data analytics, have the potential to transform agricultural practices and support the development of sustainable food production systems. Comprehensive data acquisition plays a fundamental role in this process, as it underpins informed decision-making. Access to accurate and real-time information enables farmers to adopt data-driven strategies that improve resource efficiency, increase crop productivity, and enhance environmental sustainability [27]. Big data analytics enables the transformation of heterogeneous datasets into actionable knowledge, supporting site-specific management, improving resource efficiency, facilitating predictions of crop development and associated risks, and enabling targeted agronomic interventions [28]. Furthermore, recognizing data as a strategic asset may enhance competitive positioning and support operational excellence in agricultural systems [29]. In this context, data analysis, taking into account yield and growth parameters as well as remote sensing, is an excellent tool to support the optimization of raspberry cane density for a given cultivar in specific growing conditions. This treatment can also determine not only the quality of the obtained crop, but also the ease of harvesting, the effectiveness of protection treatments, and the pressure of insect pests and pathogens. Moreover, spectral data obtained using drones can facilitate the optimization of fertilization and biostimulation for a given cane density.

The main limitations of these studies were the lack of examination of the effect of shoot density control on the nutritional and health-promoting values of fruits, plant health, and economic analysis. Future research should also focus on incorporating hyperspectral imaging and thermal imaging, and extending the study to include other cultivars, including the primocane raspberry.

5. Conclusions

This study demonstrated that cane density is a key determinant of yield formation in floricane raspberry cultivars, primarily through its strong influence on fruit number, while fruit size remains largely governed by seasonal factors. The results confirm the existence of a consistent trade-off between individual cane productivity and total yield, highlighting cane density as a central component of canopy management strategies.

The integration of multispectral imaging provided additional insight into canopy structure and its temporal dynamics, revealing that agronomic practices are reflected not only in yield parameters but also in measurable spectral responses. Although the effect of cane density on vegetation indices was moderate and variable, the combined analysis of spatial variability and temporal patterns enabled a more comprehensive characterization of plant responses than conventional field measurements alone. These findings indicate that effective raspberry production should be approached as a system-level process, in which canopy architecture, yield formation, and spectral characteristics are closely interconnected. In this context, remote sensing technologies offer a powerful tool for linking plant structure with functional responses, supporting more precise and data-driven management decisions.

The increasing availability of high-resolution multispectral data, combined with advanced analytical methods, creates new opportunities for optimizing agronomic practices, including cane density regulation, fertilization, and biostimulation strategies. The presented approach contributes

 doi:10.20944/preprints202604.1152.v1

to the development of precision horticulture by demonstrating how the combination of traditional agronomic experiments with remote sensing can improve the understanding and management of complex crop systems.

Author Contributions: Conceptualization, K.B., M.K.; methodology, K.B., M.K.; software, K.B.; validation K.B., M.K.; formal analysis, K.B., M.K.; investigation, K.B., M.K.; resources, K.B., M.K; data curation, K.B.; writing—original draft preparation, K.B.; writing—review and editing, K.B., M.K.; visualization, K.B.; supervision, K.B., M.K.; project administration, K.B., M.K.; funding acquisition, K.B., M.K.

Data Availability Statement: The multispectral data and full results are available in a public repository: https://github.com/kamilczynski/Effects-of-Cane-Density-on-Floricane-Raspberry-Assessed-Using-UAV-Based-Multispectral-Imaging (accesed on 31 March 2026).

Conflicts of Interest: The authors declare no conflicts of interest.

References

1. Bezerra, M.; Ribeiro, M.; Cosme, F.; Nunes, F.M. Overview of the Distinctive Characteristics of Strawberry, Raspberry, and Blueberry in Berries, Berry Wines, and Berry Spirits. *Comp Rev Food Sci Food Safe* **2024**, *23*, e13354, doi:10.1111/1541-4337.13354.
2. Buczyński, K.; Kapłan, M.; Jarosz, Z. Review of the Report on the Nutritional and Health-Promoting Values of Species of the Rubus L. Genus. *Agriculture* **2024**, *14*, 1324, doi:10.3390/agriculture14081324.
3. Food and Agriculture Organization of the United Nations (FAO). Available at: https://www.fao.org/faostat/en/#data/qcl (Accessed on 2 January 2026).
4. Smolarz, K. Uprawa Roślin Jagodowych Poszczególnych Gatunków. In *Sadownictwo i Szkółkarstwo*; Kijańska, I., Bujnowska, Z., Eds.; PWRiL: Warszawa, 1995; pp. 248–255.
5. Smolarz, K.; Danek, J. Maliny i Jeżyny. In *Pomologia Odmianoznawstwo Roślin Sadowniczych*; Rejman, A., Ed.; PWRiL: Warszawa, 1994; pp. 521–553.
6. Dai, W.; Hermanson, A.L.; Zhang, Q. Effects of Cane Density on Plant Growth and Fruit Production in Floricane Raspberry in the Upper Northern Climate. *hortte* **2025**, *35*, 831–833, doi:10.21273/horttech05674-25.
7. Savini, G. Raspberry Primocane and Floricane Genotype, Different Plant Types, and Fruit Cycle Manipulation. *Acta Hortic.* **2025**, 131–134, doi:10.17660/ActaHortic.2025.1444.18.
8. Merz, M.; Pedro, D.; Skliros, V.; Bergenhem, C.; Himanka, M.; Houge, T.; Matos-Carvalho, J.P.; Lundkvist, H.; Cürüklü, B.; Hamrén, R.; et al. Autonomous UAS-Based Agriculture Applications: General Overview and Relevant European Case Studies. *Drones* **2022**, *6*, 128, doi:10.3390/drones6050128.
9. Haq, S.I.U.; Wang, G.; Khan, S.N.; Song, C.; Ma, C.; Zhang, X.; Lan, Y. Multi-Dimensional Optical Remote Sensing in Agriculture: Spectral, Angular, and Spatial Scaling for Crop Stress Monitoring. *Smart Agricultural Technology* **2025**, *12*, 101583, doi:10.1016/j.atech.2025.101583.
10. Baryshnikova, N.; Altukhov, P.; Naidenova, N.; Shkryabina, A. Ensuring Global Food Security: Transforming Approaches in the Context of Agriculture 5.0. *IOP Conf. Ser.: Earth Environ. Sci.* **2022**, *988*, 032024, doi:10.1088/1755-1315/988/3/032024.
11. Bergier, I.; Barbedo, J.G.A.; Bolfe, É.L.; Romani, L.A.S.; Inamasu, R.Y.; Massruhá, S.M.F.S. Framing Concepts of Agriculture 5.0 via Bipartite Analysis. *Sustainability* **2024**, *16*, 10851, doi:10.3390/su162410851.
12. Zhang, X.; Bi, P.; Zhou, Q.; Liu, L.; Ren, L.; Luo, Y. Monitoring of Yellow Leaf Disease (YLD) Damage Based on Ground-Based LiDAR and UAV Multispectral Data. *Computers and Electronics in Agriculture* **2025**, *236*, 110461, doi:10.1016/j.compag.2025.110461.
13. Lu, R.; Park, B. Introduction. In *Hyperspectral Imaging Technology in Food and Agriculture*; Park, B., Lu, R., Eds.; Food Engineering Series; Springer New York: New York, NY, 2015; pp. 3–7 ISBN 978-1-4939-2835-4.
14. Rejeb, A.; Abdollahi, A.; Rejeb, K.; Treiblmaier, H. Drones in Agriculture: A Review and Bibliometric Analysis. *Computers and Electronics in Agriculture* **2022**, *198*, 107017, doi:10.1016/j.compag.2022.107017.
15. Kondraju, T.T.; Sahoo, R.N.; Ramalingam, S.; Rejith, R.G.; Bhandari, A.; Ranjan, R.; Reddy, D.V.S.C. Exploring the Application of UAV-Multispectral Sensors for Proximal Imaging of Agricultural Crops. In

 doi:10.20944/preprints202604.1152.v1

Proceedings of the The 12th International Electronic Conference on Sensors and Applications; MDPI, November 7 2025; p. 91.

16. ElHalawany, B.M.; Alshammeri, S.; Aldaihani, S.; Alyouhah, M.; Alrashidi, R. Drone-Aided Agriculture 5.0: A Survey on Machine-Learning and IoT Paradigms for Smart Farming. In *Proceedings of the 2nd Symposium on Smart, Sustainable, and Secure Internet of Things*; Trabelsi, M., Khan, M., Bouida, Z., Murugappan, M., Eds.; Lecture Notes in Electrical Engineering; Springer Nature Singapore: Singapore, 2026; Vol. 1513, pp. 53–64 ISBN 9789819551354.
17. Azlan, Z.H.Z.; Junaini, S.N.; Khan, A.S.; Mustafa, W.A. Data-Driven Agriculture: Unveiling the Power of Internet of Things and Data Analytics For Transformative Farming Practices. *Journal of Sensors* **2025**, *2025*, 6205646, doi:10.1155/js/6205646.
18. DJI Agriculture. Available Online: https://ag.dji.com/mavic-3-m (Accessed on 20 October 2025).
19. Processing Options Pix4Dfields. Available Online: https://support.pix4d.com/hc/en-us/articles/360028421272#label7 (Accessed on 20 November 2025).
20. Kamilczynski. GitHub Repository 2026. Available Online: https://github.com/kamilczynski/effects-of-cane-density-on-primocane-raspberry-assessed-using-uav-based-multispectral-imaging (Accessed on 14 February 2026).
21. Buczyński, K.; Kapłan, M.; Jarosz, Z. Effects of Cane Density on Primocane Raspberry Assessed Using UAV-Based Multispectral Imaging. *Agriculture* **2026**, *16*, 742, doi:10.3390/agriculture16070742.
22. Kamilczynski. GitHub Repository 2026. Available Online: https://github.com/kamilczynski/effects-of-cane-density-on-floricane-raspberry-assessed-using-uav-based-multispectral-imaging (Accessed on 31 March 2026).
23. Oliveira, P.B.; Oliveira, C.M.; Monteiro, A.A. Pruning Date and Cane Density Affect Primocane Development and Yield of `Autumn Bliss' Red Raspberry. *HortSci* **2004**, *39*, 520–524, doi:10.21273/HORTSCI.39.3.520.
24. Ciebień, M.; Rachoń, L. Ocena Plonowania Malin Odmian Powtarzających Owocowanie w Zależności Od Zagęszczenia Pędów w Rzędach w Warunkach Padołu Zamojskiego. *Agron. Sci.* **2023**, *78*, 55–68, doi:10.24326/as.2023.4600.
25. Nes, A.; Hageberg, B.; Haslestad, J.; Hagelund, R. INFLUENCE OF CANE DENSITY AND HEIGHT ON PRODUCTIVITY AND PERFORMANCE OF RED RASPBERRY (RUBUS IDAEUS L.) CULTIVAR "GLEN AMPLE." *Acta Hortic.* **2008**, 231–236, doi:10.17660/ActaHortic.2008.777.34.
26. Životić, A.; Mićić, N.; Žabić, M.; Bosančić, B.; Cvetković, M. Precision Cane Meristem Management Can Influence Productivity and Fruit Quality of Floricane Red Raspberry Cultivars. *Turk J Agric For* **2019**, *43*, 405–413, doi:10.3906/tar-1807-15.
27. Weraikat, D.; Šorič, K.; Žagar, M.; Sokač, M. Data Analytics in Agriculture: Enhancing Decision-Making for Crop Yield Optimization and Sustainable Practices. *Sustainability* **2024**, *16*, 7331, doi:10.3390/su16177331.
28. Ahanou, Z.; Mrabti, F.; Dhassi, Y. Big Data Analytics in Precision Agriculture: An Automated Systematic Literature Review. *Computers and Electronics in Agriculture* **2026**, *243*, 111401, doi:10.1016/j.compag.2025.111401.
29. Uyar, H.; Karvelas, I.; Rizou, S.; Fountas, S. Data Value Creation in Agriculture: A Review. *Computers and Electronics in Agriculture* **2024**, *227*, 109602, doi:10.1016/j.compag.2024.109602.